

Supporting Information

Discovery of a Bioactive Inhibitor with a New Scaffold for Cystathionine γ -Lyase

Youtian Hu,^{†,#} Lu Wang,^{‡,#} Xu Han,^{§,#} Yueyang Zhou,[†] Tonghui Zhang,[†] Li Wang,[†]
Ting Hong,^{†,||} Wei Zhang,[⊥] Xun-Xiang Guo,[†] Jieli Sun,[†] Yingxin Qi,[‡] Jing Yu,^{⊥,*}
Hong Liu,^{§,*} Fang Wu^{†,*}

[#]These authors contributed equally.

Table of Contents

EXPERIMENTAL SECTION	S2
Figure S1. The optimization and validation of the HTS assay for hCSE	S13
Figure S2. The validation and structural basis of NSC267461 for the inhibition of hCSE.	S15
Figure S3. Enzyme kinetics of hCSE WT and mutants.	S17
Figure S4. MS and NMR spectra of the trimethyl NSC4056.	S18
Figure S5.	S22
Figure S6. NSC4056 inhibits the cellular H ₂ S in Raw264.7 macrophages	S24
Figure S7. The effects of NSC4056 on the level of H ₂ S in HEK293T expressing of hCSE WT or mutants	S26
Figure S8. The effects of NSC4056 on the level of H ₂ S in HEK293T expressing of hCBS WT.	S28
Figure S9. Effects of NSC4056 on the cell viability of Raw264.7 macrophages or HEK293T cells.	S29
Table S1. Chemical structures and IC ₅₀ values of top 10 potent CSE inhibitors	S30
Table S2. The IC ₅₀ and K _i values of NSC4056 on hCSE wild-type and mutants in the <i>in vitro</i> purified enzyme assay.	S32
Table S3. Primer sequences.	S33
References	S34

1. EXPERIMENTAL SECTION

1.1 Compound Library. The compound library used in our study contains 11,954 agents including 2,635 synthetic compounds from the National Cancer Institute (NCI; Bethesda, MD), 1,563 from the US Food and Drug Administration (FDA) or Foreign Approved Drugs (FAD)-approved drugs from the Johns Hopkins Clinical Compound Library (JHCCL, Baltimore, MD),¹ 4,406 natural products from AnalytiCon Discovery (Potsdam, Germany), 800 natural products and 2,180 clinical compounds from TargetMol (Boston, MA), and 370 commercially available synthetic compounds or natural products from Specs (Delft, Netherlands), ChemDiv (San Diego, CA), ChemBridge (San Diego, CA) or PI & PI Technology (Guangzhou, Guangdong, China).

1.2 Plasmids. Human CSE (hCSE) and human CBS-413 (hCBS-413, a fully active truncated form of hCBS) were cloned into the pGEX-KG empty vector to generate the N-terminal GST-fusion proteins as previously described.² Human dopa decarboxylase (hDDC) was inserted into the His-Tag fusion plasmid pET28b.³ For the protein expression in mammalian cells, hCSE or hCBS-FL was cloned into the pCDH-CMV vector in the EcoR I and Not I sites. The R62A, R62K, Y114A, Y114F, R119A, R119K, N241A and N241K hCSE mutants were generated from pGEX-KG-hCSE or pCDH-CMV-hCSE templates using PCR using primers 1-2, 3-4, 5-6, 7-8, 9-10, 11-12, 13-14 and 15-16, respectively. All of the plasmids were subsequently confirmed by DNA sequencing.

1.3 Expression and Purification. The pGEX-KG plasmids carrying the WT or

mutant hCSEs were transformed into *E. coli* BL21-CodonPlus cells and affinity purified with GST agarose (Proteintech, Chicago, IL) according to the procedures detailed in previous studies.² The eluted GST-tagged proteins were collected, aliquoted and stored at -80 °C.

1.4 High-throughput Screening Assay for hCSE. The CSE high-throughput (HTS) assay was constructed based on a 192-tandem-well plate.² The HTS campaign for CSE inhibitors was carried out by a Beckman Biomek FXP liquid handling system (Beckman Coulter Inc., Brea, CA). Briefly, 25 µl 50 mM HEPES buffer containing 500 nM hCSE and 100 µM PLP (final concentrations; pH 7.4) was first incubated with 1 µL DMSO or compounds at a concentration of 10 or 100 µM for 45 min. Then, 50 µl detection buffer (300 µM DTNB in 262 mM Tris-HCl and 13 mM EDTA, pH 8.9) was added into the interlinked well. Finally, 25 µl 50 mM HEPES buffer containing 5 mM L-Cys (final concentrations) was added in the reaction well and the plate was immediately and tightly sealed with UltraClear film (Platemax PCR-TS from Axygen, Union City, CA). The assay plate was then incubated for 60 min at 37 °C before the absorbance was measured at 413 nm with a microplate reader (Cytation5 from BioTek, Winooski, VT).

1.5 IC₅₀ and K_i of Inhibitors for hCSE, hCBS and hDDC. The IC₅₀ values of 30 hits as well as analogs of NSC4056 were determined for WT hCSE or hCSE mutants for at least eight inhibitor concentrations (0-200 µM). Briefly, WT hCSE (500 nM), R62A (10 µM), R62K (5 µM), Y114A (5 µM), Y114F (1.25 µM), R119K (1.25 µM), R119A (1.25 µM), N241A (1.25 µM) and N241K (1.25 µM) were respectively mixed

with 0.4 mM L-Cys for the R62A, Y114A and Y114F mutants, 2 mM L-Cys for the R62K mutant, 3 mM L-Cys for the N241A mutant, 4 mM L-Cys for the N241K mutant, 5 mM L-Cys for the WT hCSE and R119K mutant, or 7 mM L-Cys for the R119A mutant, which approximately corresponded to the determined K_m values (Figure S3). The IC_{50} value was obtained by fitting the plot with a four-parameter logistic equation in SigmaPlot 9 (Systat Software, Erkrath, Germany). The competitive K_i values for NSC4056 or NSC267461 were calculated with the Cheng-Prusoff equation for competitive inhibitors.⁴

The IC_{50} values of the CSE inhibitors for hCBS-413 and hDDC were determined under standard assay conditions as previously described.^{2, 3}

The experiments were performed at least twice and a representative experiment is shown.

1.6 H₂S-donor Counterscreen Assay. To exclude the possibility that inhibitors react with the H₂S generated during the enzymatic assay, a counterscreen assay was constructed with NaHS, a commonly-used H₂S donor, based on a reported setting.⁵ Briefly, 1 μ L inhibitor at indicated concentrations was added together with 500 μ M NaHS (final concentration) into the reaction well of the tandem-well plate, which contains only the HEPES assay buffer. The DTNB was then added into the coupled detection well before an immediate seal of the plate. The sealed assay plate was incubated for 40 min at 37 °C before the absorbance at 413 nm was measured. The experiments were performed at least twice and a representative experiment is shown.

1.7 Quantitative Analysis of Homocysteine via LC/ESI-MS/MS. The effect of NSC4056 on the level of Hcys in the *in vitro* purified CSE assay was determined by a liquid chromatography-tandem mass spectrometry (LC/ESI-MS/MS). We followed the condition for Hcys MS detection that has been established previously.⁶ The singly charged parent ion for Hcys was observed at 136 m/z. The product ion scan showed dominant product ions at m/z values of 118 and 90. We selected the 136 → 90 transition for the quantitative method. Briefly, ten microliters of the collected samples were applied to the Ultra Performance Liquid Chromatographic system on a Zorbax XDB C18 reverse phase column (4.6 × 150 mm, temperature-controlled at 16 °C), and eluted with acetonitrile supplemented with 0.1% formic acid and water with 0.1% formic acid (50:50, v/v) at a flow rate of 0.4 ml/min in a diode array detector (Agilent G4212A). The Agilent 6470 UHPLC-QqQ/MS system composes of a chromatographic system (Agilent 1260 Infinity) and a Triple Quad mass spectrometer fitted with an ESI source. Data was acquired in the MRM mode using Agilent MassHunter Workstation Data Acquisition Software (revision B.04). The experiments were performed twice and a representative experiment is shown.

1.8 Reversibility Assay. The binding reversibility of NSC4056 and NSC267461 to hCSE was tested by rapid dilution of the enzyme-bound inhibitor with assay buffer.⁷ Briefly, 20 μM hCSE was incubated with 20 μM NSC4056, 100 μM NSC267461 or 100 μM PAG for 40 min in 50 mM HEPES (pH 7.4). Then, the enzyme-inhibitor complex was diluted 200-fold into the hCSE assay buffer (50 mM HEPES, 5 mM L-Cys and 100 μM PLP; pH 7.4). At 0, 1, 2 or 4 h post-dilution, the CSE activity was measured according to the standard hCSE assay conditions (see above). The experiments were performed at least twice and a representative experiment is shown.

1.9 Enzyme Kinetics. The mode of inhibition by NSC4056 and NSC267461 was analyzed with a Michaelis-Menten model and Lineweaver-Burk analysis.^{7, 8} Briefly, the hCSE reaction rate was determined with the indicated concentrations of NSC4056 or NSC267461 against increasing concentrations of PLP (0-15 mM in the presence of 25 mM L-Cys) or L-Cys (0-100 mM in the presence of 100 μ M PLP). The kinetic data were transformed into Lineweaver-Burk plots to illustrate the type of inhibition (competitive, noncompetitive or mix type inhibition). The inhibition constant K_i was obtained by fitting the plots of the initial velocity versus the concentration of PLP or L-Cys with a nonlinear competitive inhibition equation using GraphPad Prism 5 (San Diego, CA). The experiments were performed at least twice and a representative experiment is shown.

1.10 PLP Absorption and Fluorescence Assay. The effect of NSC4056 on the interaction between PLP and CSE was determined by monitoring the absorbance spectra and fluorescence emission spectra of the bound PLP across 350 nm to 450 nm or at 509 nm under an excitation of 412 nm with previously developed methods.^{9, 10} Briefly, various concentrations of NSC4056 were incubated with 12.5 μ M hCSE in the presence of 50 mM HEPES (pH 7.4), and the absorbance (350-450 nm) and emission spectra (425-650 nm) were collected with a Nanodrop 2000c spectrophotometer (Thermo Scientific, Wilmington, DE) by using a quartz microcuvette and a microplate reader (Cytation5 from BioTek, Winooski, VT), respectively.

1.11 Isothermal Titration Calorimetry. ITC experiments were done on the MicroCal iTC200 system (GE Healthcare) at 25 °C. NSC4056, NSC267461 and hCSE protein were prepared in 50 mM Tris-HCl (pH 7.5) containing 2% DMSO. The inhibitor (0.5 mM) was injected in 2- μ L aliquots and for 20 times into the calorimetric

cell filled with 0.22 mM hCSE. Raw calorimetric data were corrected for the heat of dilution, and analyzed with Origin 6.0 software for ITC version 6.0 (MicroCal). Binding stoichiometry, enthalpy and equilibrium dissociation constants were determined by fitting the corrected data into the single binding site model. The experiments were performed twice and a representative experiment is shown.

1.12 Molecular Docking. The crystal structure of the hCSE, PAG and PLP complex (PDB code: 3COG) was obtained from the RCSB Protein Data Bank (<http://www.rcsb.org/>).¹¹ The structures of NSC4056 and NSC267461 were obtained from PubChem (<http://pubchem.ncbi.nlm.nih.gov/>). The hCSE complex structure was removed from the inhibitor PAG and prepared as a target for inhibitor docking studies with the Discovery Studio software (version 3.5; Accelrys, San Diego, CA). After energy minimization, NSC4056 or NSC267461 was docked into the hCSE active site using the CDOCKER module in Discovery Studio.

1.13 The Synthesis of Trimethyl Ester of NSC4056. NSC4056 and TMSCHN₂ [(trimethylsilyl)diazomethane solution] were purchased from Alfa Aesar (Ward Hill, MA). The other materials were obtained from Sigma-Aldrich unless otherwise indicated. ¹H and ¹³C nuclear magnetic resonance spectra (NMR) were acquired on a Bruker 400 MHz or 500 MHz NMR spectrometer (Bruker BioSpin, Billerica, MA). Chemical shifts (δ) were expressed in ppm using tetramethylsilane as an internal reference and the coupling constants (*J*) were indicated in Hz. The coupling constants were described as singlet (s), doublet (d), triplet (t), quartet (q), quintet (quint), broad (br) or multiplet (m). HRMS data was obtained on an Agilent G6520 Q-TOF with Electrospray Ionization (ESI). Preparative HPLC data was collected on a Waters

AutoPurification HPLC System.

NSC4056 (3.0 g, 7.1 mmol) was first dissolved with CHCl_3 (50 ml) and MeOH (25 ml) in a 250 ml flask. TMSCHN_2 (2 N in hexane solution, 36 ml, 71 mmol) was added dropwise to the reaction mixture over 15 min. The resulting mixture was stirred at ambient temperature for 2 h and the reaction process was monitored by TLC. Another amount of TMSCHN_2 (2 N in hexane solution, 20 ml) was supplemented and the mixture was kept stirring at ambient temperature for 12 h. The reaction was subsequently quenched with some drops of AcOH and solvent was removed *in vacuo*. The crude product was first purified by flash column chromatography on silica gel (200-300 mesh) eluting with EtOAc (EA)/petroleum ether (PE) (1:10, v/v, $R_f = 0.6$) and further purified by preparative HPLC to afford the corresponding compound as an orange solid. ^1H NMR (400 MHz, $\text{DMSO}-d_6$) δ 10.50 (s, 3H), 7.69 (d, $J = 2.4$ Hz, 3H), 7.26 (dd, $J = 8.4, 2.4$ Hz, 3H), 6.95 (d, $J = 8.8$ Hz, 3H), 3.84 (s, 9H); ^{13}C NMR (125 MHz, $\text{DMSO}-d_6$) δ 169.5, 159.3, 138.8, 135.5, 129.0, 117.4, 112.7, 79.4, 52.9; LR-MS (ESI): $m/z = 464.8$ $[\text{M} + \text{H}]^+$; HRMS: m/z : $[\text{M} + \text{H}]^+$ calculated for $\text{C}_{25}\text{H}_{21}\text{O}_9$: 465.1180, found 465.1181.

1.14 The Redox Activity Assay. The redox activity of NSC4056 was determined by a previously developed horseradish peroxidase (HRP) -phenol red assay.¹² Briefly, the assay was performed in a 384-well-plate with the assay buffer (PBST; 0.01% Triton X-100 in 25 mM Na_3PO_4 , pH 7.0). For testing the compound, 1 μL compound was mixed with 39 μL assay buffer in the absence or the presence of DTT (final concentration: 1 mM) and the mixture was incubated for 15 min at room temperature.

Then, 20 μ L solution (280 μ M HRP, 60 μ g/mL phenol red in the assay buffer) was added into the assay and the reaction was incubated at room temperature for additional 30 min. Finally, the assay was terminated by adding 10 μ L of 1 M NaOH, and the absorbance of the phenol red was measured at 610 nm in the plate reader (Synergy2 from BioTek, Winooski, VT). According to the established standard, the tested compounds with a background-subtracted absorbance (correction via subtracting the absorbance of DMSO-only sample) above 0.2 are considered as redox-active compounds.¹²

1.15 Cells. Raw264.7 cell line was originally obtained from the Shanghai Cell Bank (Chinese Academy of Science, Shanghai, China). HEK293T cells were kindly gifted by Dr. H. Gehring (University of Zurich, Zurich, Switzerland). Raw264.7 and HEK293T cells were cultured in DMEM (Gibco, Grand Island, NY), with 10% FBS and 1% penicillin and streptomycin in a 5% CO₂ incubator at 37 °C.

1.16 Stable Cell Lines. HEK293T were seeded into 10-cm dishes and co-transfected with lentivirus transfer vectors (pCDH-CMV vector carrying CSE, CSE-Y114F, CSE-R119A, CSE-R119A or CBS) and pPACK Packaging Plasmid Mix (SBI, MZIPxxxPA-1) according to the manufacturer's instructions. For infection of HEK293T cells and Raw264.7 cells, cells were infected with lentiviruses carrying the corresponding gene in the presence of 8 μ g/ml polybrene. After 48 h transduction, cells were selected by 2.5 μ g/ml puromycin-containing medium for at least two weeks to obtain stable clones.

1.17 H₂S Imaging in Cells. To quantify the H₂S in cells, AzMC probe, an H₂S-specific fluorescent probe,^{13, 14} was employed and a reported staining procedure

was followed. Briefly, Raw264.7 or HEK293T cells WT or stably expressing of WT, mutant CSE or CBS were seeded on poly-D-Lys-coated cover slips (Thermo Scientific, Waltham, MA) in a 12-well plate for 24 h. Subsequently, the cells were treated with inhibitors or DMSO for 12 h. Then, the cells were washed at least three times with PBS buffer and fixed with 4% paraformaldehyde for 10 min. The fixed cells were stained with 50 μ M 7-azido-4-methylcoumarin (AzMC) in the dark and at 37 °C for 30 min before taking the fluorescent images with an excitation wavelength of 380 nm under a confocal laser scanning fluorescence microscopy (A1Si, Nikon, Tokyo, Japan). The intensity of the blue fluorescent signals, which indicate the amount of H₂S, was quantified with the ImageJ software (National Institutes of Health, NIH, Bethesda, MD). The H₂S signal was subtracted by the background signal detected in HEK293T cells stably expressing the empty vector (HEK293T-EV), normalized with the corresponding cell area and compared with the control (DMSO group, 100%; Figure 4A). Similarly, the H₂S signal in Raw264.7 cells was quantified by AzMC staining, corrected for the background signal outside the cells, normalized by the cell area and expressed as percentages of DMSO control (100%, Figure 3A). The experiments were performed at least twice and a representative experiment is shown.

1.18 Lead Acetate Assay for Detection of Volatile H₂S Generated by Cells. To detect the effect of NSC4056 or PAG on the cell-released H₂S in HEK293T cells or Raw264.7 macrophages stably expressing of WT CSE, CSE mutants or CBS, a standard protocol was followed.¹⁵ Briefly, the cells were seeded at 1×10^6 cells/well in 96-well-plates for a day. Then, cells were incubated with fresh-prepared culture-medium containing 50 mM L-Cys and NSC4056 or PAG at indicated concentrations. The lead acetate strips (SSS Reagent Ltd., Shanghai, China) were put

on the wells to detect the cell-released H₂S. After a further incubation of 24 h, the lead acetate papers were taken out and the blackness in the strip (PbS) was visually inspected. The experiments were performed at least twice and a representative experiment is shown.

1.19 Rat Hemorrhagic Shock Model. Sprague-Dawley rats (7 weeks in age, 250-300 g body weight, male) for the hemorrhagic shock model were purchased from Vital River Laboratory Animals (Beijing, China). The animals were maintained on a daily 12 h light/dark cycle and fed a normal chow diet at room temperature (RT). All of the experiments were approved by the Animal Research Committee of Shanghai Jiao Tong University. The hemorrhagic shock rat model was constructed by withdrawing blood from the artery according to the method as previously described.¹⁶ Briefly, male rats were anaesthetized with sodium pentobarbital (40 mg/kg, i.p.). Then, the left carotid artery was exposed and cannulated with a PE-50 catheter to monitor the mean arterial pressure (MAP). After a 30 min stabilization period, blood (3 ml/100 g) was withdrawn to induce hemorrhagic shock until the MAP decreased to ~ 25 mmHg. Then, saline (0.9% w/v, 1 ml/kg) or NSC4056 (50 mg/kg) were injected intraperitoneally 30 min after blood withdrawal. MAP was monitored continuously throughout the experiment by a MP30B-CE pressure transducer (BIOPAC, Santa Barbara, CA). Forty-five min post-injection, the blood samples (1 ml) were collected to measure of the amounts of plasma H₂S and Hcys by Methylene Blue and ELISA methods, respectively.

1.20 ELISA. The amount of Hcys in the cell supernatant or rat plasma was quantified by an Axis homocysteine EIA Kit according to the standard protocol provided by the manufacturer (IBL, Gunma, Japan). The experiments were performed at least twice and a representative experiment is shown.

1.21 Quantification of H₂S by Methylene Blue Method. The amount of H₂S in the rat plasma or the *in vitro* purified CSE assay was quantified by the Methylene Blue method.^{16, 17} Briefly, aliquots of plasma (180 μ l) were mixed with zinc acetate (10% w/v, 20 μ l) to trap the H₂S before the addition of trichloroacetic acid (10% w/v, 50 μ l) to precipitate proteins in the plasma. Then, 100 μ l 20 mM *N,N*-dimethyl-p-phenylenediamine sulfate (DPD; dissolved in 7.2 M HCl) was added, followed by the addition of 100 μ l 30 mM FeCl₃ (dissolved in 1.2 M HCl). For measuring the H₂S generated by the *in vitro* purified CSE or CBS assay, 5 μ l zinc acetate (10% w/v) was added into the 50 μ l reaction solution before adding 25 μ l DPD (20 mM) and 25 μ l FeCl₃ (30 mM). After incubated for 5 min, the mixture was added with trichloroacetic acid and centrifuged to precipitate the protein. The absorbance of 50 μ l of the resulting supernatant was measured at 670 nm in a 384-well microplate by a plate reader (BioTek, Winooski, VT). The H₂S concentration of each sample was calculated from a NaHS standard curve. The experiments were performed at least twice and a representative experiment is shown.

1.22 Western Blots. The endogenous level of CSE in HEK293T or Raw264.7 cells were analyzed by Western blotting with an anti-CSE (GeneTex, San Antonio, TX) antibody.

1.23 Quantification and Statistical Analysis. Statistical analysis was performed on the raw data for each group by one-way or two-way ANOVA. A $p < 0.05$ was considered statistically significant.

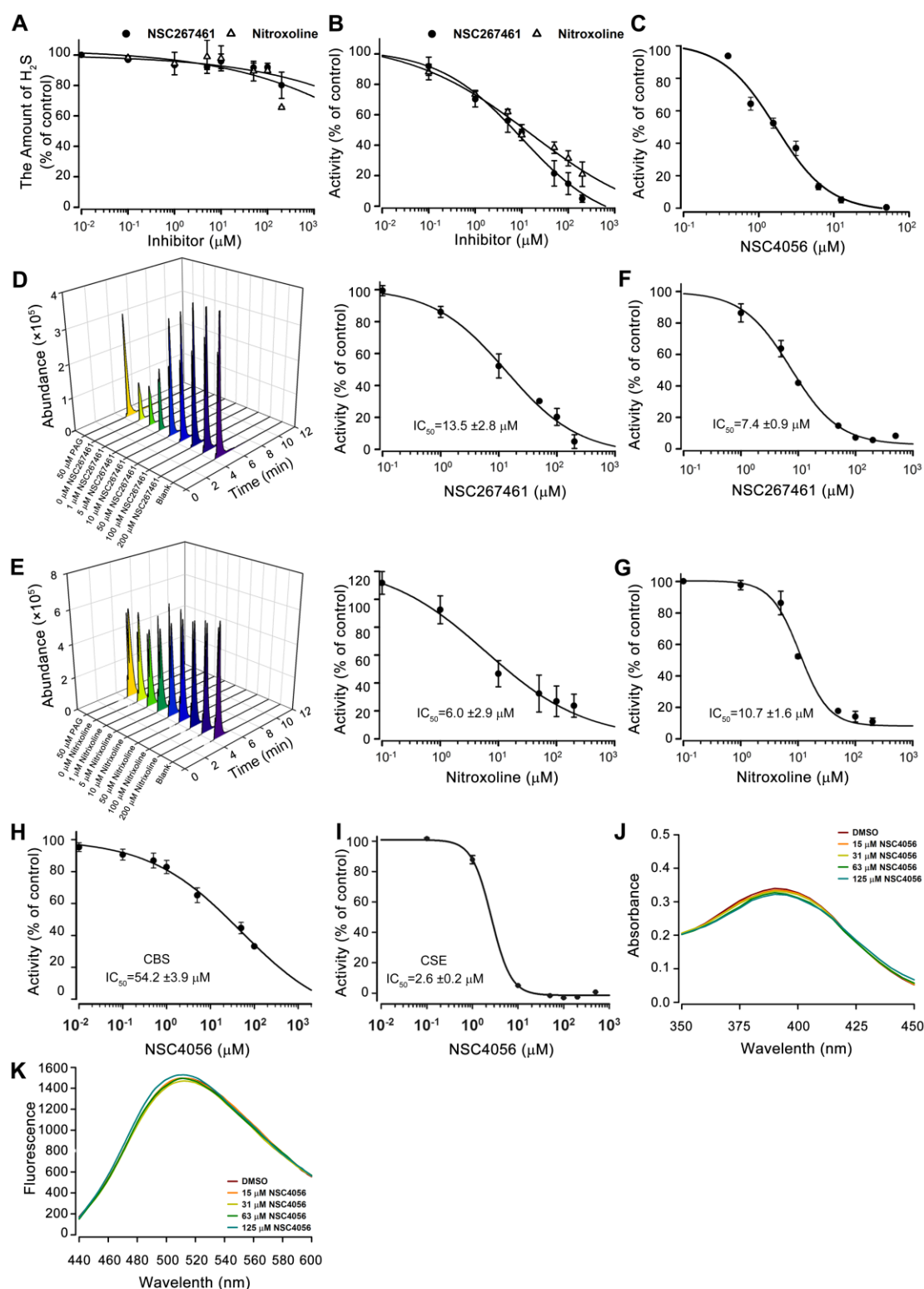


Figure S1. The optimization and validation of the HTS assay for hCSE. (A) NSC267461 or Nitroxoline does not interfere with H_2S at low-micomolar concentrations. NSC267461 or Nitroxoline at the indicated concentrations was incubated with $500 \mu M$ NaHS in the absence of the CSE at $37^\circ C$. The released H_2S was quantified by DTNB in the tandem-well. (B) The effects of nonionic detergents

on the inhibition of NSC267461 or Nitroxoline to CSE. CSE was incubated with NSC267461 or Nitroxoline at the indicated concentration in the presence of 0.01% Triton X-100, and the remaining activities were accordingly measured under the standard assay conditions (see Experimental Section). (C) Dose-dependent inhibition of NSC4056 on the amount of H₂S in the presence of 4 mM Hcys. (D-E) NSC267461 (D) and Nitroxoline (E) accumulate the Hcys substrate in the assay containing only 4 mM Hcys substrate, as analyzed by LC/ESI-MS/MS. (F-G) Dose-dependent inhibition of NSC267461 (F) and Nitroxoline (G) on the amount of H₂S in the presence of 4 mM Hcys. (H-I) Dose-dependent inhibition of NSC4056 for hCBS (H) and hCSE (I) as analyzed with the Methylene Blue method (see Experimental Section). (J-K) NSC4056 does not influence the binding site of PLP in CSE as revealed by analyzing the absorbance (J) and fluorescence spectra (K) of PLP. The data are expressed as percentages of the control (DMSO, 100%) and presented as mean \pm S.D (n = 4, for A-C; n = 3, for F-K; n = 2, for D and E). The absorbance of NSC4056 interferes with the absorbance spectrum of PLP between 250 nm and 350 nm, therefore, the absorbance across 350 nm and 450 nm of PLP is only shown. All experiments were performed at least twice and a representative experiment is shown.

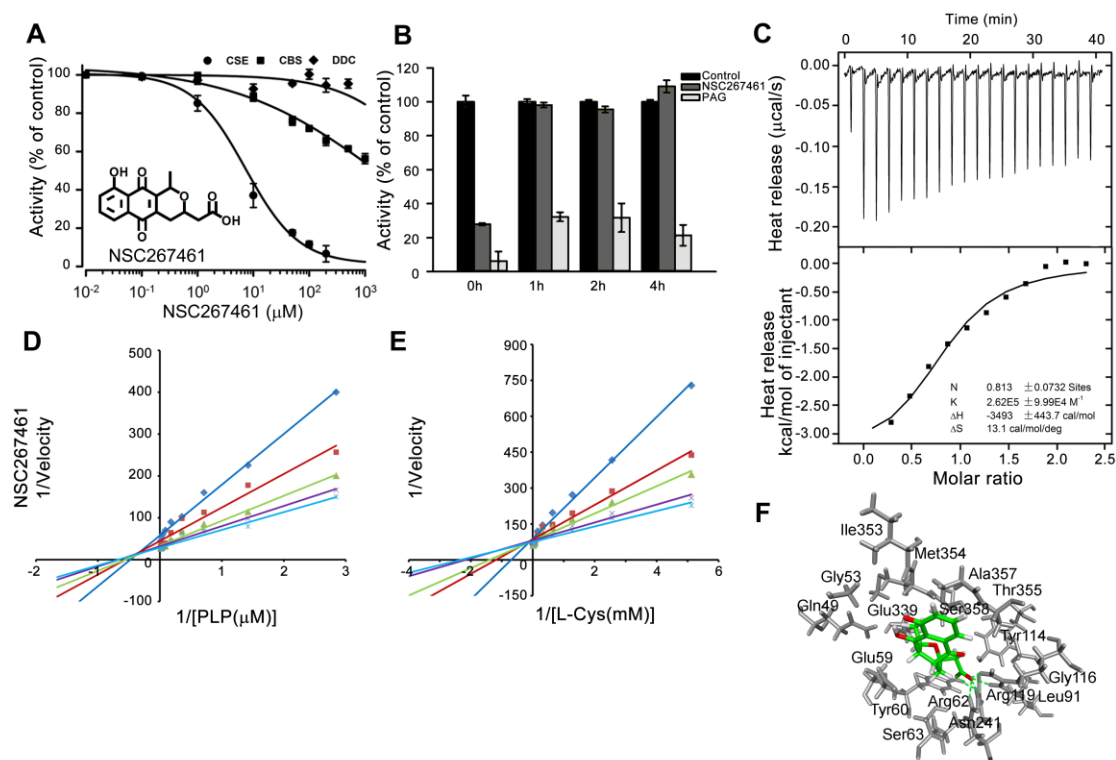


Figure S2. The validation and structural basis of NSC267461 for the inhibition of hCSE. (A) Dose-dependent inhibition of NSC267461 for hCSE (●), hCBS (■) and hDDC (◆). The data (n = 4) are expressed as percentages of the control (DMSO, 100%) and presented as mean ± S.D. (B) NSC267461 inhibits hCSE in a reversible manner. After incubation with 100 μM NSC267461 or 100 μM PAG for 40 min, hCSE (20 μM) was diluted 200-fold in assay buffer and incubated for additional 1, 2 or 4 h before adding 5 mM Cys substrate to start the enzyme reaction. The activities were measured at each time point and are expressed as percentages of the control (DMSO, 100%). The data are presented as mean ± S.D. (n = 4). (C) Isothermal titration calorimetry assay to confirm the direct binding between NSC267461 and hCSE. Upper, raw data; lower, the releasing heat was fitted into the single binding site model. (D) Inhibition of hCSE by NSC267461 as a function of PLP concentration with L-Cys (20 mM) as a substrate (non-competitive inhibition $\alpha K_i = 15.2 \pm 1.1 \mu\text{M}$). (E) Inhibition of hCSE by NSC267461 as a function of L-Cys concentration in the presence of PLP (100 μM) (competitive inhibition constant $K_i = 4.9 \pm 0.7 \mu\text{M}$). Each point in the Lineweaver-Burk plots represents the average of duplicates. The αK_i and K_i values were calculated using the non-linear fitting method for enzyme kinetics with

GraphPad Prism 5. (F) The putative binding mode of NSC267461 in the hCSE active site. NSC267461 was docked into the hCSE crystal structure (PDB code 3COG) using the Discovery Studio software. Residues surrounding the inhibitor within a distance of 5 Å are shown in gray; NSC267461 is in green and by default atom type (O and N), and hydrogen bonds are represented as green dotted lines. All of the experiments were performed at least twice and a representative experiment is shown.

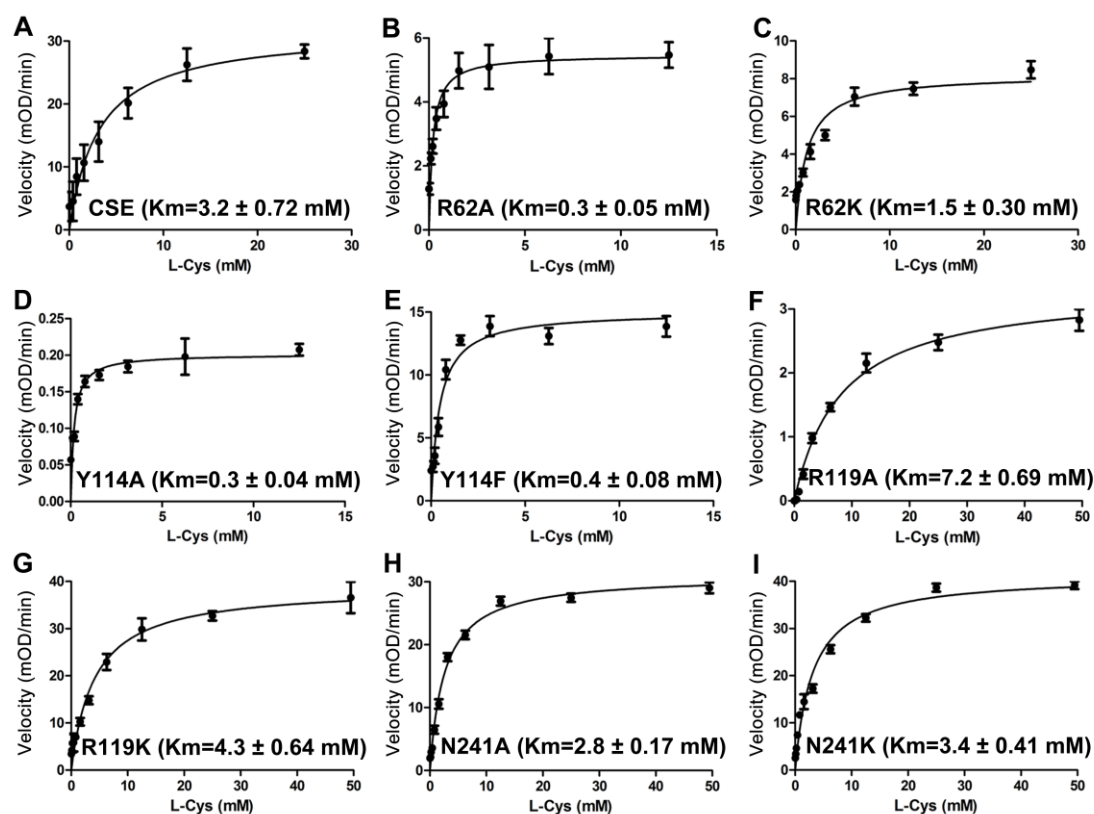
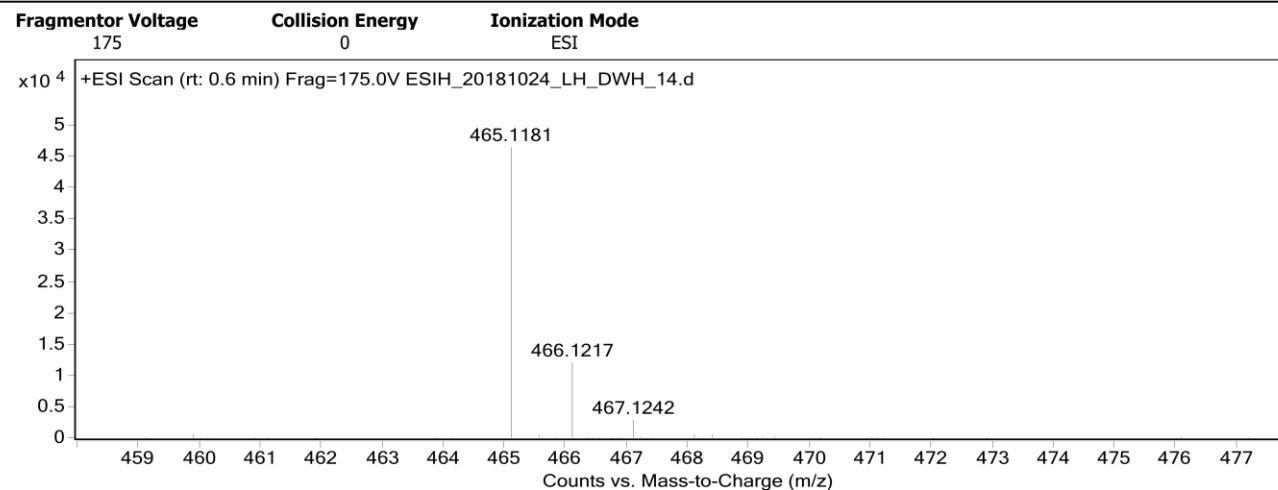


Figure S3. Enzyme kinetics of hCSE WT and mutants. The kinetic curve for hCSE was determined by incubating 500 nM hCSE WT and mutants with the various concentrations of L-Cys (0, 0.391, 0.781, 1.563, 3.125, 6.25, 12.5, 25 or 50 mM) under the standard assay conditions described in Experimental Section. The reaction velocity (mOD/min) was accordingly calculated (see above) and the K_m was obtained by fitting the data into the Michaelis-Menten equation. Data were presented as mean \pm S.D. ($n = 4$). The experiments were performed twice and a representative data is shown.

Qualitative Analysis Report

Data Filename	ESI_H_20181024_LH_DWH_14.d	Sample Name	B6-ATAOCH3
Sample Type	Sample	Position	P1-C3
Instrument Name	Agilent G6520 Q-TOF	Acq Method	20160322_MS_ESI_H_POS_1min.m
Acquired Time	10/24/2018 19:30:12	IRM Calibration Status	Success
DA Method	small molecular data analysis method.m	Comment	ESI_H by ZZY

User Spectra

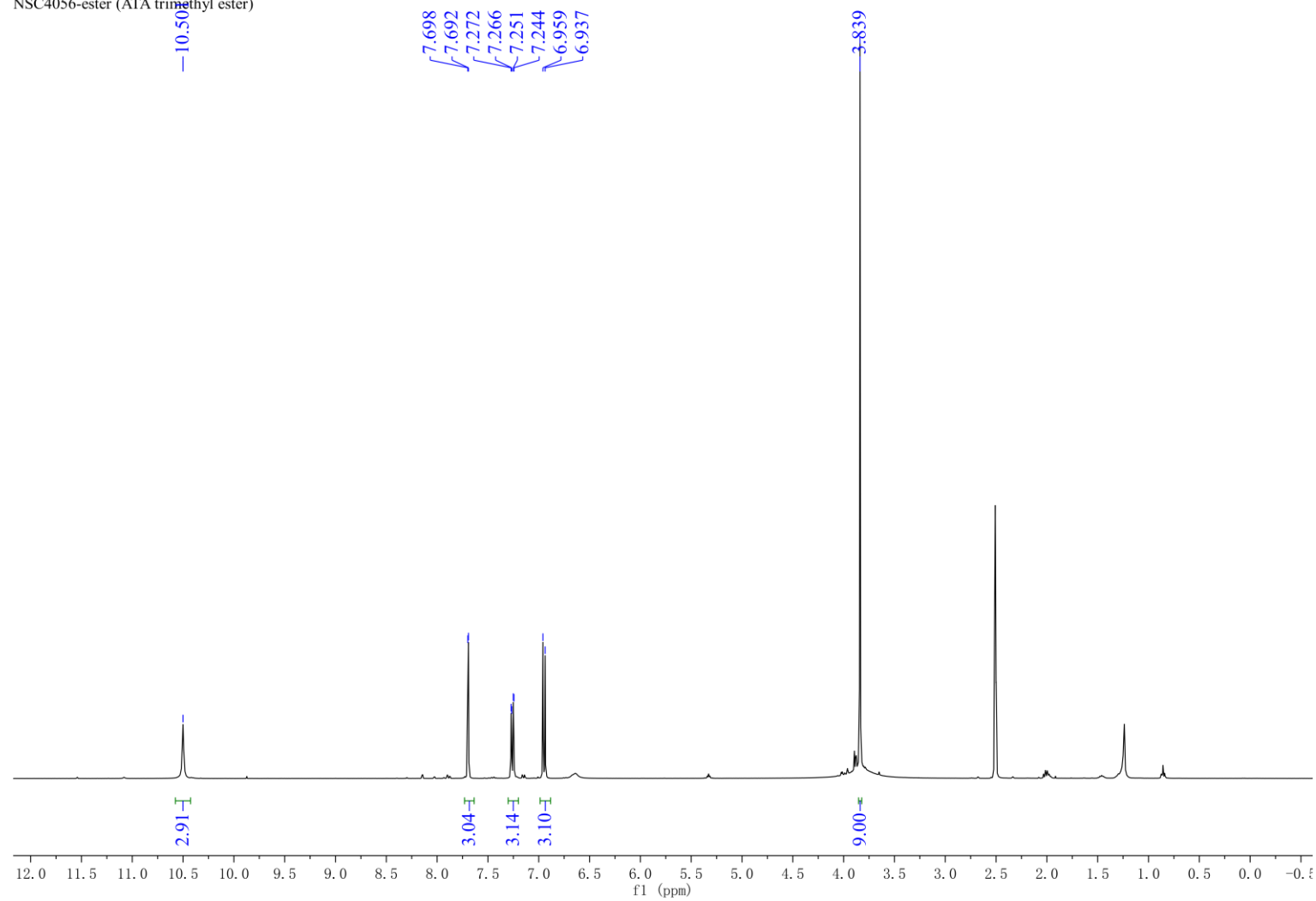


Formula Calculator Results

m/z	Calc m/z	Diff (mDa)	Diff (ppm)	Ion Formula	Ion
465.1181	465.118	-0.1	-0.22	C25 H21 O9	(M+H)+

--- End Of Report ---

NSC4056-ester (ATA trimethyl ester)



NSC4056-ester (ATA trimethyl ester)

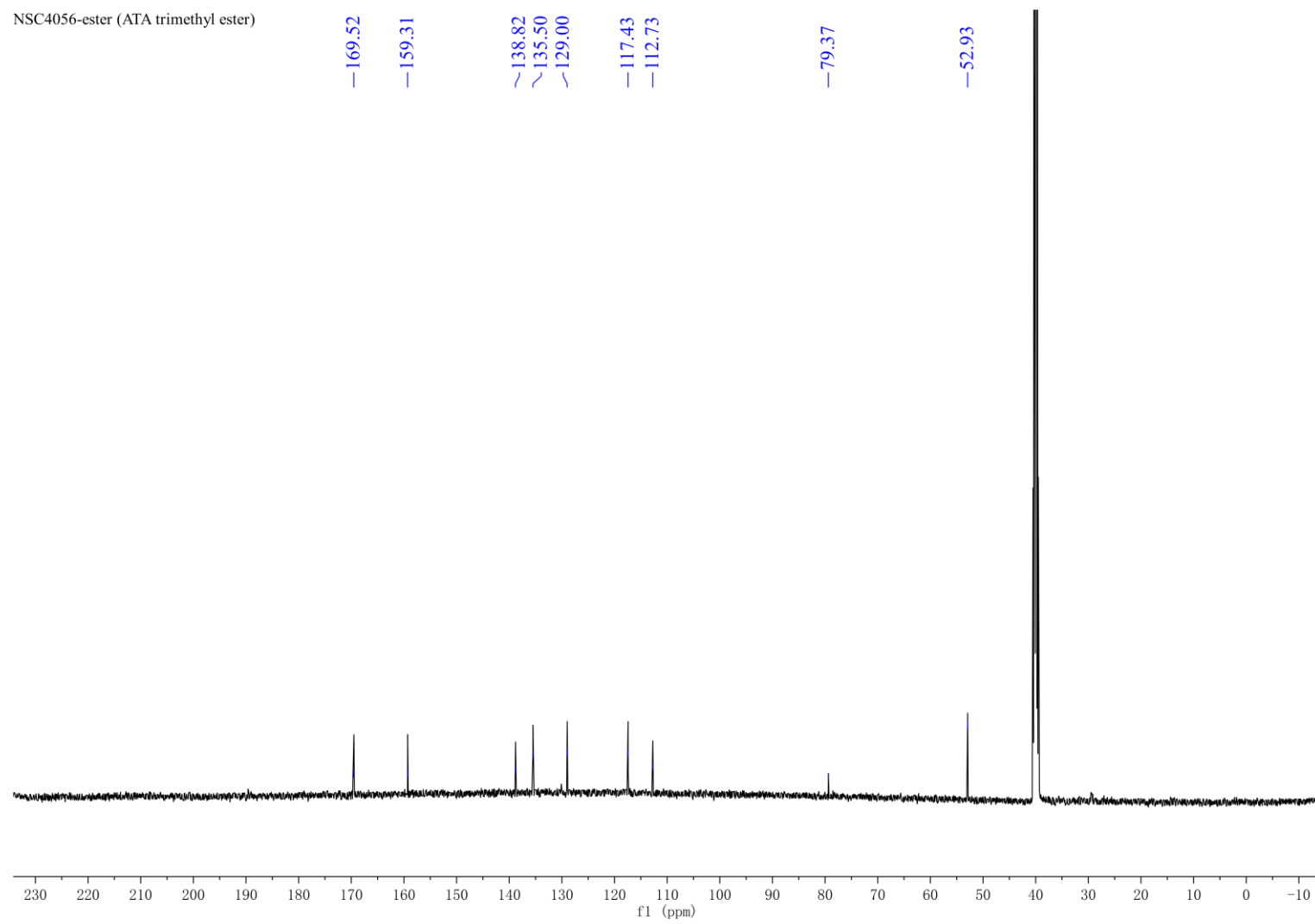


Figure S4. MS and NMR spectra of the trimethyl NSC4056. (A) HR-ESI-MS spectra of trimethyl NSC4056. The molecular formula of $C_{25}H_{21}O_9$ was deduced from a $[M+H]^+$ ion peak at m/z 465.1181 in the HR-ESI-MS, which is consistent with the calculated molecular weight for $[M+H]$, 465.118. (B) 1H NMR spectra of trimethyl NSC4056 (400 MHz, DMSO- d_6) δ 10.50 (s, 3H), 7.69 (d, $J = 2.4$ Hz, 3H), 7.26 (dd, $J = 8.4, 2.4$ Hz, 3H), 6.95 (d, $J = 8.8$ Hz, 3H), 3.84 (s, 9H). (C) ^{13}C NMR spectra of trimethyl NSC4056 (125 MHz, DMSO- d_6) δ 169.5, 159.3, 138.8, 135.5, 129.0, 117.4, 112.7, 79.4, 52.9.

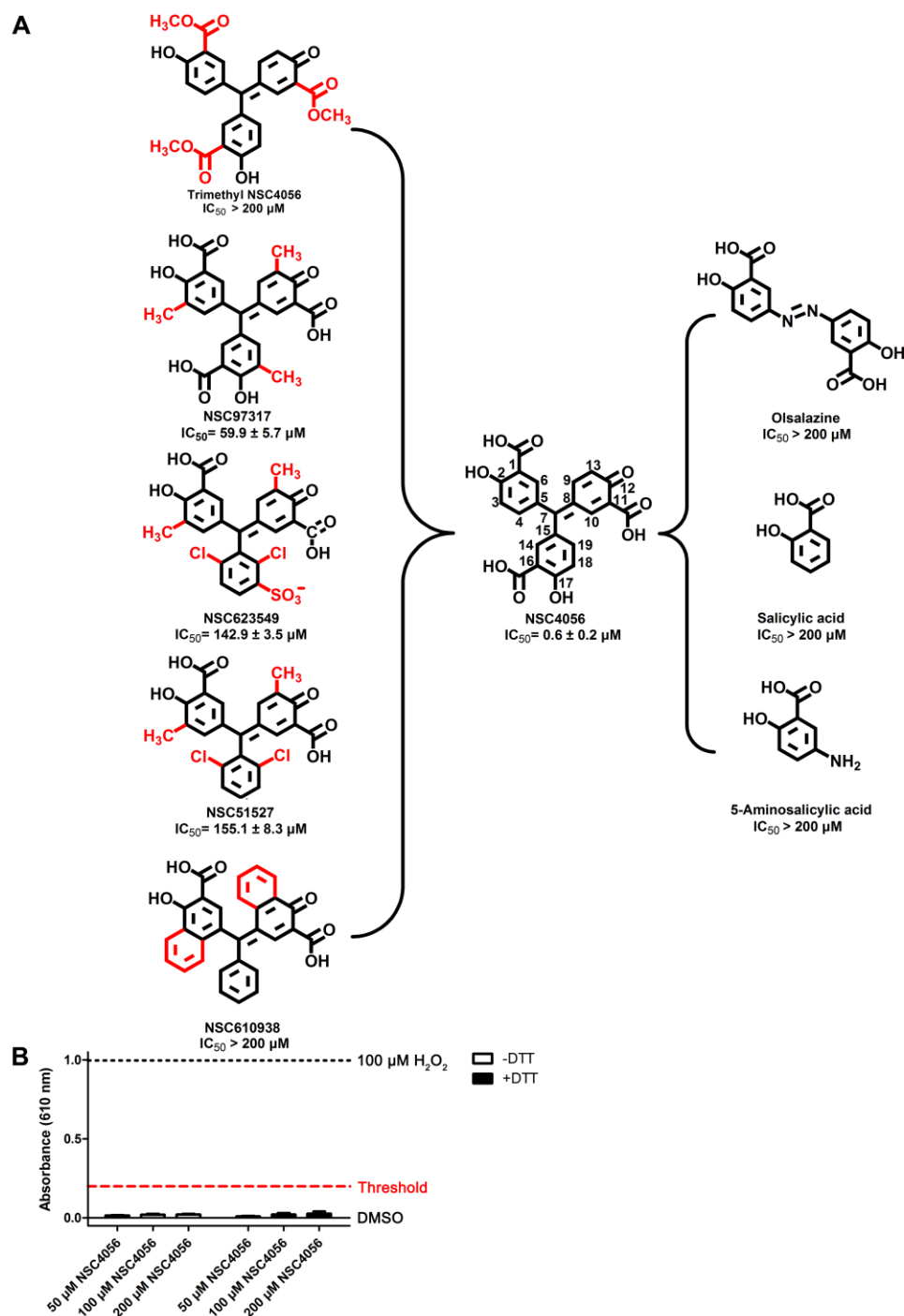


Figure S5. (A) Chemical structures and IC_{50} values for the analogs of NSC4056. Structure analogs of NSC4056, i.e. trimethyl NSC4056, NSC97317, NSC623549, NSC51527 or NSC610938 (left), as well as fragments of NSC4056, i.e. olsalazine, salicylic acid or 5-aminosalicylic acid (right), were included in the structure-activity relationship study. The inhibitory effects of these compounds were determined in the hCSE assay under the standard conditions (see Experimental Section). (B) The redox activities of NSC4056 in the the absence or the presence of the reducing agent DTT.

NSC4056 at indicated concentrations (50, 100 or 200 μM) was assayed according to a standard protocol by using a modified horseradish peroxidase-phenol red assay (for details, please see Experimental Section).¹² H_2O_2 at a concentration of 100 μM was used as the positive control (black dash line). Compound with an absorbance above 0.2 (red dash line) is identified as a redox-active compound. Data are showed as mean \pm S.D. ($n = 3$). All of the experiments were performed at least twice.

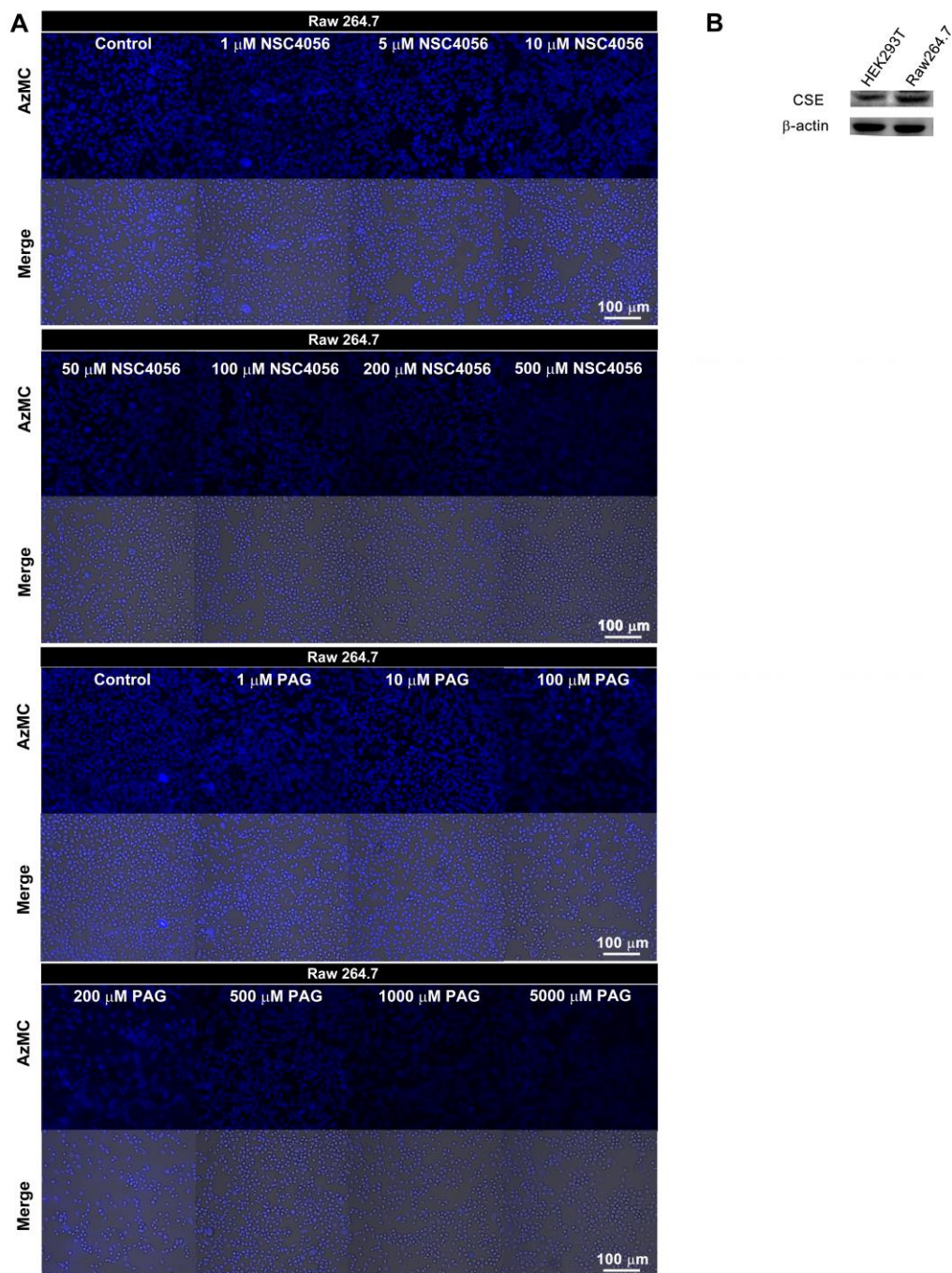


Figure S6. NSC4056 inhibits the cellular H₂S in Raw264.7 macrophages. (A) NSC4056 dose-dependently suppresses the H₂S level in Raw264.7 macrophages. Raw264.7 cells were treated with indicated concentrations of NSC4056 or PAG for 12 h before the incubation with 50 μ M AzMC for 30 min at 37 °C. The fluorescent images of H₂S (blue) or bright-field images of cells were taken under a Nikon-A1Si confocal microscope at 20 \times magnification. AzMC image, H₂S image (blue); Merge, the overlapped image of H₂S and bright-field image for the cells. Bars, 100 μ m.

Typical images and quantification data for the H₂S level were additionally displayed in Figure 3A. (B) Expression levels of endogenous CSE in HEK293T and Raw264.7 cells. ~ 10 µg of respective cell lysate was subjected to 10% SDS-PAGE for analyzing of the level of CSE by Western Blot using an anti-CSE antibody (GeneTex). All experiments were performed at least two times and a representative experiment is shown.

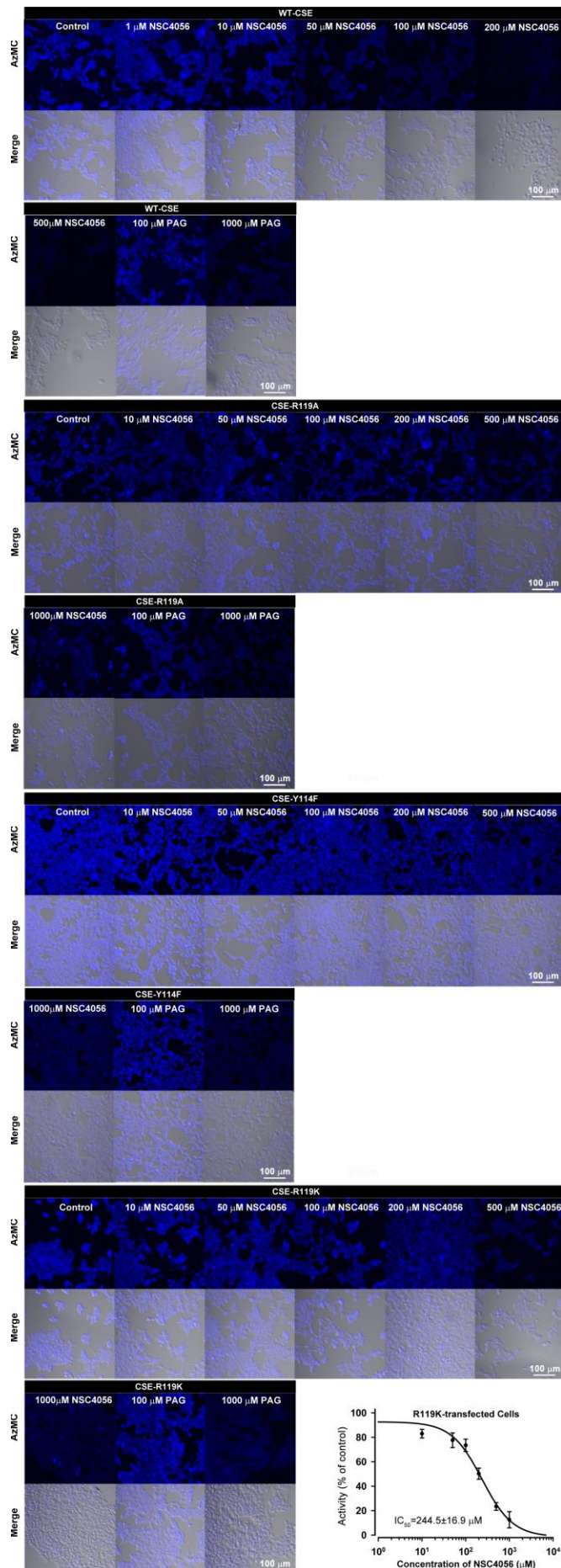


Figure S7. The effects of NSC4056 on the level of H₂S in HEK293T expressing of hCSE WT or mutants. HEK293T cells stably expressing WT CSE, CSE-R119A, CSE-Y114F or CSE-R119K were seeded for 24 h before the treatment with indicated concentrations of NSC4056 or PAG for 12 h. The content of H₂S was measured with 50 μ M AzMC as described above. Images were taken using the confocal microscope. AzMC image, H₂S image (blue); Merge, the overlapped image of H₂S and bright-field image for the cells. Typical images were additionally displayed in Figure 4A. The amount of H₂S in HEK293T cells expressing of WT CSE, CSE-R119A, CSE-Y114F or CSE-R119K with the treatment of various concentrations of NSC4056 (0-1000 μ M) was quantified and subtracted with the background signals by analyzing the blue images with ImageJ software according to the procedures described in Experimental Section. Bars, 100 μ m. The data are expressed as percentages of DMSO control (100%) and displayed in Figure 4A or in the present figure. Data were presented as mean \pm S.D. (n = 4). All experiments were performed at least twice and a representative experiment is shown.

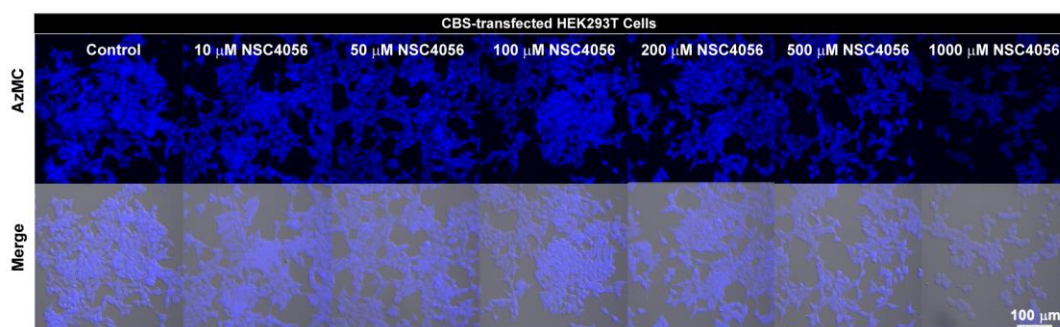


Figure S8. The effects of NSC4056 on the level of H₂S in HEK293T expressing of hCBS-FL. HEK293T cells stably expressing of hCBS-FL were seeded for 24 h before the treatment with indicated concentrations of NSC4056 for 12 h. The content of H₂S was measured with 50 μ M AzMC as described above. Images were taken using the confocal microscope. AzMC image, H₂S image (blue); Merge, the overlapped image of H₂S and bright-field image for the cells. The amount of H₂S in HEK293T cells expressing of hCBS with the treatment of various concentrations of NSC4056 (0-1000 μ M) was quantified and subtracted with the background signals by analyzing the blue images with ImageJ software according to the procedures described in Experimental Section. Typical images and quantification data for the H₂S level were additionally displayed in Figure 4A. Bars, 100 μ m. The data are expressed as percentages of DMSO control (100%). Mean \pm S.D. (n = 4). All experiments were performed at least twice and a representative experiment is shown.

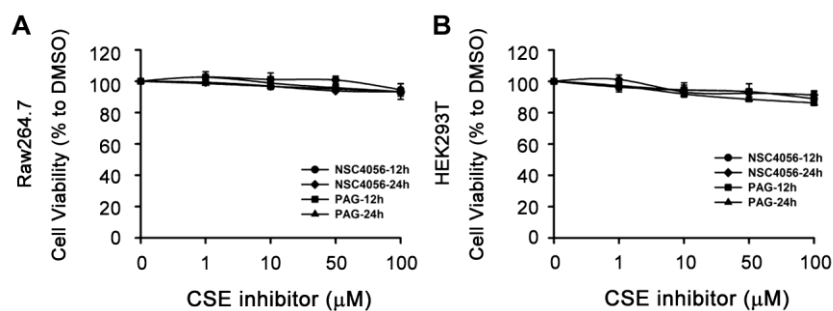
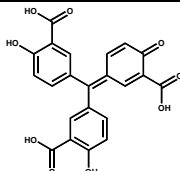
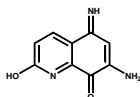
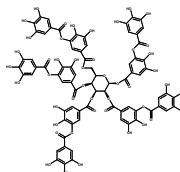
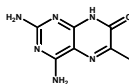
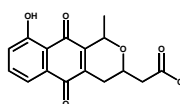
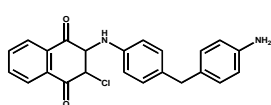
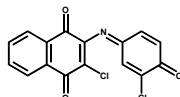
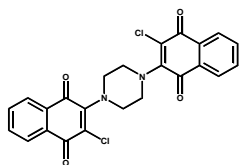
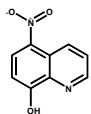
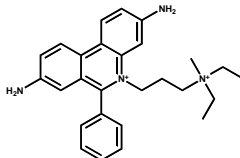


Figure S9. Effects of NSC4056 on the cell viability of Raw264.7 macrophages or HEK293T cells. Raw264.7 (A) macrophages or HEK293T cells (B) were seeded in 96-well plates at a density of 6,000 cells/well for a day before the treatment with various concentrations of NSC4056 or PAG (a known inhibitor for CSE) for 12 or 24 h. Then, the cell viability was measured by using the CellTiter96 Aqueous One Solution Cell Proliferation Assay (Promega). The means at each concentration were shown as percentages of the DMSO control (100%). Means \pm S.D. (n = 4).

Table S1. Chemical structures and IC₅₀ values of top 10 potent CSE inhibitors

Name	Structure	IC ₅₀ (μM)			Selectivity: IC ₅₀ (hCBS-413) /IC ₅₀ (hCSE)	Selectivity: IC ₅₀ (hDDC)/ IC ₅₀ (hCSE)
		hCSE	hCBS-413 ^a	hDDC		
NSC4056 (Aurintricarboxylic acid; ATA)		0.6 ± 0.2 2.6 ± 0.2 ^c 1.7 ± 0.3 ^d 3.3 ± 0.6 ^e	82.6 ± 2.9 54.2 ± 3.9 ^c	> 100 ^b	137.7	> 142.6
NSC111041 ^f		2.5 ± 0.1	4.0 ± 0.5	35.0 ± 1.7	1.6	14
Glycerite		5.6 ± 1.3	3.6 ± 0.1	>500	0.6	>89.2
NSC33414		6.1 ± 0.2	22.6 ± 2.5	> 200	3.7	> 32.8
NSC267461		6.2 ± 0.9 7.4 ± 0.9 ^d 13.5 ± 2.8 ^e	> 1000	> 200	> 161.3	> 32.3
AH-034/32861052		7.5 ± 1.4	15.4 ± 1.7	> 200	2.1	> 26.7
AE-848/08322020		7.6 ± 2.3	22.1 ± 3.8	> 200	2.9	> 26.3
NSC40341		7.9 ± 0.6	30.5 ± 5.3	> 200	3.9	> 25.3
Nitroxoline		8.0 ± 2.8 10.7 ± 1.6 ^d 6.0 ± 2.9 ^e	>500	>100 ^b	>62.5	>12.5
Propidium Iodide		9.0 ± 1.3	12.1 ± 2.0	>200	1.3	>22.2

^ahCBS-413, a fully active truncated form of hCBS.

^bNSC4056 and Nitroxoline at a concentration of more than 100 μM have substantial absorbance at 340 nm that interferes with the activity measurement for hDDC.

^cThe IC₅₀ of NSC4056 on CSE and CBS-413 were also determined using the Methylene Blue Method.

^dThese IC₅₀ values were determined using 4 mM Hcys as a substrate under standard assay conditions.

^eThese IC₅₀ values in the assay (d) were also determined by the accumulation of Hcys, which is quantified by LC/ESI-MS/MS.

^fNSC111041 was initially identified by us and the IC₅₀ values of it for hCSE, hCBS or hDDC were previously obtained.²

Table S2. The IC₅₀ and K_i values of NSC4056 on hCSE wild-type and mutants in the *in vitro* purified enzyme assay.

Enzymes	K _m	L-Cys mM	IC ₅₀ μM	Selectivity: IC ₅₀ (MUT)/ IC ₅₀ (WT)	K _i ^a μM	Selectivity: K _i (MUT)/K _i (WT)
WT	3.2 ± 0.72	5	0.6 ± 0.2	1.0	0.2 ± 0.1	1.0
R62A	0.3 ± 0.05	0.4	6.7 ± 1.2	11.1	2.2 ± 0.4	11
R62K	1.5 ± 0.30	2	12.9 ± 1.5	21.5	5.6 ± 0.6	28
Y114A	0.3 ± 0.04	0.4	10.2 ± 1.2	17.1	3.8 ± 0.5	19
Y114F	0.4 ± 0.08	0.4	17.8 ± 2.3	29.6	8.9 ± 1.1	44.5
R119A	7.2 ± 0.69	7	19.2 ± 2.3	32.0	10.4 ± 1.2	52
R119K	4.3 ± 0.64	5	15.6 ± 2.8	26.0	8.1 ± 1.5	40.5
N241A	2.8 ± 0.17	3	2.5 ± 0.5	4.1	1.2 ± 0.2	6
N241K	3.4 ± 0.41	4	4.4 ± 1.1	7.3	1.7 ± 0.4	8.5

^aThe inhibition constant K_i value of competitive inhibitor NSC4056 for L-Cys was calculated from the IC₅₀ value by using Cheng-Prusoff equation for competitive inhibitor: $IC_{50}=K_i \times (1 + \frac{[S]}{K_m})$, among which [S] is the concentration of L-Cys used in the dose-dependent assay (Figure 2F and Experimental Section) and K_m is the Michaelis-Menten constant of L-Cys (Figure S3).⁴

Table S3. Primer Sequences.

No.	Primer	Usage
1	5'-GCACTCGGGTTTTGAATATAGCGCTTCTGGAAATCCCACTAGGAATTGCC-3'	5' primer for constructing CSE-R62A mutant
2	5'-GGCAATTCCTAGTGGGATTTCCAGAAGCGCTATATTCAAAACCCGAGTGC-3'	3' primer for constructing CSE-R62A mutant
3	5'-GCACTCGGGTTTTGAATATAGCAAGTCTGGAAATCCCACTAGGAATTGCC-3'	5' primer for constructing CSE-R62K mutant
4	5'-GGCAATTCCTAGTGGGATTTCCAGACTTGCTATATTCAAAACCCGAGTGC-3'	3' primer for constructing CSE-R62K mutant
5	5'-CCAAATTATTTGTATGGATGATGTGGCTGGAGGTACAAACAGGTACTTCAGGC-3'	5' primer for constructing CSE-Y114A mutant
6	5'-GCCTGAAGTACCTGTTTGTACCTCCAGCCACATCATCCATACAAATAATTTGG-3'	3' primer for constructing CSE-Y114A mutant
7	5'-CCAAATTATTTGTATGGATGATGTGTTGGAGGTACAAACAGGTACTTCAGGC-3'	5' primer for constructing CSE-Y114F mutant
8	5'-GCCTGAAGTACCTGTTTGTACCTCCAAACACATCATCCATACAAATAATTTGG-3'	3' primer for constructing CSE-Y114F mutant
9	5'-GGATGATGTGTATGGAGGTACAAACGCGTACTTCAGGCAAGTGGCATCTG-3'	5' primer for constructing CSE-R119A mutant
10	5'-CAGATGCCACTTGCCTGAAGTACGCGTTTGTACCTCCATACACATCATCC-3'	3' primer for constructing CSE-R119A mutant
11	5'-GGATGATGTGTATGGAGGTACAAACAAGTACTTCAGGCAAGTGGCATCTG-3'	5' primer for constructing CSE-R119K mutant
12	5'-CAGATGCCACTTGCCTGAAGTACTTGTGTTGTACCTCCATACACATCATCC-3'	3' primer for constructing CSE-R119K mutant
13	5'-GCCTTCATAATAGACTTCGTTTCTTGCAAGCCTCTCTTGGAGCAGTCCATCTCCTATTGATTG-3'	5' primer for constructing CSE-N241A mutant
14	5'-CAATCAATAGGAGATGGAAGTCTCCAAGAGAGGCTTGCAAGAAACGAAGTCTATTATGAAGGC-3'	3' primer for constructing CSE-N241A mutant
15	5'-GCCTTCATAATAGACTTCGTTTCTTGCAAAAATCTCTTGGAGCAGTCCATCTCCTATTGATTG-3'	5' primer for constructing CSE-N241K mutant
16	5'-CAATCAATAGGAGATGGAAGTCTCCAAGAGATTTTGTGCAAGAAACGAAGTCTATTATGAAGGC-3'	3' primer for constructing CSE-N241K mutant

References

- (1) Chong, C. R.; Sullivan, D. J., Jr. New uses for old drugs. *Nature* **2007**, *448*, 645-646.
- (2) Zhou, Y.; Yu, J.; Lei, X.; Wu, J.; Niu, Q.; Zhang, Y.; Liu, H.; Christen, P.; Gehring, H.; Wu, F. High-throughput tandem-microwell assay identifies inhibitors of the hydrogen sulfide signaling pathway. *Chem. Commun. (Camb)*. **2013**, *49*, 11782-11784.
- (3) Ren, J.; Zhang, Y.; Jin, H.; Yu, J.; Zhou, Y.; Wu, F.; Zhang, W. Novel inhibitors of human DOPA decarboxylase extracted from *Euonymus glabra* Roxb. *ACS. Chem. Biol.* **2014**, *9*, 897-903.
- (4) Cheng, Y.; Prusoff, W. H. Relationship between the inhibition constant (K₁) and the concentration of inhibitor which causes 50 per cent inhibition (I₅₀) of an enzymatic reaction. *Biochem. Pharmacol.* **1973**, *22*, 3099-3108.
- (5) Druzhyna, N.; Szczesny, B.; Olah, G.; Modis, K.; Asimakopoulou, A.; Pavlidou, A.; Szoleczky, P.; Gero, D.; Yanagi, K.; Toro, G.; Lopez-Garcia, I.; Myrianthopoulos, V.; Mikros, E.; Zatarain, J. R.; Chao, C.; Papapetropoulos, A.; Hellmich, M. R.; Szabo, C. Screening of a composite library of clinically used drugs and well-characterized pharmacological compounds for cystathionine beta-synthase inhibition identifies benzerazide as a drug potentially suitable for repurposing for the experimental therapy of colon cancer. *Pharmacol. Res.* **2016**, *113*, 18-37.
- (6) Nelson, B. C.; Pfeiffer, C. M.; Sniegowski, L. T.; Satterfield, M. B. Development and evaluation of an isotope dilution LC/MS method for the determination of total homocysteine in human plasma. *Anal. Chem.* **2003**, *75*, 775-784.
- (7) Purich, D. L. *Enzyme Kinetics Catalysis and Control*. First edition ed.; Elsevier Inc.: London, 2010; p 485-537.
- (8) Stein, R. L. *Kinetics of Enzyme Action: Essential Principles for Drug Hunters*. John Wiley & Sons Singapore, 2011.
- (9) Campanini, B.; Speroni, F.; Salsi, E.; Cook, P. F.; Roderick, S. L.; Huang, B.; Bettati, S.; Mozzarelli, A. Interaction of serine acetyltransferase with O-acetylserine sulfhydrylase active site: evidence from fluorescence spectroscopy. *Protein Sci.* **2005**, *14*, 2115-2124.
- (10) Spyraakis, F.; Singh, R.; Cozzini, P.; Campanini, B.; Salsi, E.; Felici, P.; Raboni, S.; Benedetti, P.; Cruciani, G.; Kellogg, G. E.; Cook, P. F.; Mozzarelli, A. Isozyme-specific ligands for O-acetylserine sulfhydrylase, a novel antibiotic target. *PloS one* **2013**, *8*, e77558.
- (11) Sun, Q.; Collins, R.; Huang, S.; Holmberg-Schiavone, L.; Anand, G. S.; Tan, C. H.; van-den-Berg, S.; Deng, L. W.; Moore, P. K.; Karlberg, T.; Sivaraman, J. Structural basis for the inhibition mechanism of human cystathionine gamma-lyase, an enzyme responsible for the production of H₂S. *J. Biol. Chem.* **2009**, *284*, 3076-3085.
- (12) Dahlin, J. L.; Nelson, K. M.; Strasser, J. M.; Barsyte-Lovejoy, D.; Szewczyk, M. M.; Organ, S.; Cuellar, M.; Singh, G.; Shrimp, J. H.; Nguyen, N.; Meier, J. L.; Arrowsmith, C. H.; Brown, P. J.; Baell, J. B.; Walters, M. A. Assay interference and off-target liabilities of reported histone acetyltransferase inhibitors. *Nat. Commun.* **2017**, *8*, 1527.
- (13) Thorson, M. K.; Majtan, T.; Kraus, J. P.; Barrios, A. M. Identification of cystathionine beta-synthase inhibitors using a hydrogen sulfide selective probe. *Angew. Chem. Int. Ed. Engl.* **2013**, *52*, 4641-4644.
- (14) Chen, B.; Li, W.; Lv, C.; Zhao, M.; Jin, H.; Du, J.; Zhang, L.; Tang, X. Fluorescent probe for highly selective and sensitive detection of hydrogen sulfide in living cells and cardiac tissues. *Analyst* **2013**, *138*, 946-951.
- (15) Hine, C.; Harputlugil, E.; Zhang, Y.; Ruckenstein, C.; Lee, B. C.; Brace, L.; Longchamp, A.; Trevino-Villarreal, J. H.; Mejia, P.; Ozaki, C. K.; Wang, R.; Gladyshev, V. N.; Madeo, F.; Mair, W. B.; Mitchell, J. R. Endogenous hydrogen sulfide production is essential for dietary restriction benefits. *Cell* **2015**, *160*, 132-144.
- (16) Mok, Y. Y.; Atan, M. S.; Yoke Ping, C.; Zhong Jing, W.; Bhatia, M.; Mochhala, S.; Moore, P. K. Role of hydrogen sulphide in haemorrhagic shock in the rat: protective effect of inhibitors of hydrogen sulphide biosynthesis. *Br. J. Pharmacol.* **2004**, *143*, 881-889.
- (17) Bucci, M.; Vellecco, V.; Cantalupo, A.; Brancalone, V.; Zhou, Z.; Evangelista, S.; Calderone, V.; Papapetropoulos, A.; Cirino, G. Hydrogen sulfide accounts for the peripheral vascular effects of zofenopril independently of ACE inhibition. *Cardiovasc. Res.* **2014**, *102*, 138-147.